

Phase diagram of the asymmetric tetrahedral Ising–Heisenberg chain

This article has been downloaded from IOPscience. Please scroll down to see the full text article.

2008 J. Phys.: Condens. Matter 20 345208

(<http://iopscience.iop.org/0953-8984/20/34/345208>)

View [the table of contents for this issue](#), or go to the [journal homepage](#) for more

Download details:

IP Address: 129.252.86.83

The article was downloaded on 29/05/2010 at 13:56

Please note that [terms and conditions apply](#).

Phase diagram of the asymmetric tetrahedral Ising–Heisenberg chain

J S Valverde, Onofre Rojas and S M de Souza

Departamento de Ciências Exatas, Universidade Federal de Lavras, Caixa Postal 3037, CEP 37200-000, Lavras, MG, Brazil

Received 29 April 2008, in final form 18 June 2008

Published 1 August 2008

Online at stacks.iop.org/JPhysCM/20/345208

Abstract

The asymmetric tetrahedron is composed of all edges of a tetrahedron represented by Ising interactions except for one, which has a Heisenberg-type interaction. This asymmetric tetrahedron is arranged by connecting a vertex whose edges are only Ising-type interactions to another vertex with the same structure for another tetrahedron. The process is replicated and this kind of lattice we call the asymmetric Ising–Heisenberg chain. We have studied the ground-state phase diagram for this kind of model. In particular, we consider two situations in the Heisenberg-type interaction: (i) the asymmetric tetrahedral spin-(1/2, 1/2) Ising-XYZ chain and (ii) the asymmetric tetrahedral spin-(1/2, 1) Ising-XXZ chain, where we have found a rich phase diagram and a number of multicritical points. Additionally we have also studied their thermodynamical properties and the correlation function, using the decorated transformation. We have mapped the asymmetric tetrahedral Ising–Heisenberg chain in an effective Ising chain, and we have also concluded that it is possible to evaluate the partition function including a longitudinal external magnetic field.

1. Introduction

Low-dimensional systems based on magnetic material have attracted considerable attention lately in a number of subjects such as condensed matter physics, material science and inorganic chemistry. In these particular areas quantum ferrimagnetic chains (QFC) were discussed, due to that they exhibit a relevant combination of ferromagnetic (F) and antiferromagnetic (AF) states. Experimental synthesis of the compound $\text{Cu}(\text{3-Clpy})_2(\text{N}_3)_2$ [1], with Clpy indicating chloropyridine, had been investigated. This compound could be mapped into a spin-1/2 tetramer chain with F–F–AF–AF bond alternation [2]. Recently diamond-type chain structures have been intensively investigated theoretically and experimentally [3]. The natural candidates to describe these kinds of materials are the quantum anisotropic Heisenberg models or even Ising-type models. Certainly the rigorous mapping of those compounds into Heisenberg-type models could produce very complex systems which usually have a non-exact solution. However, some particular cases of models could become exactly solvable, such as the Ising–Heisenberg model considered by Jascur and Strecka [4], see also a more detailed discussion considered by Canova *et al* [5]. The method used to solve this kind of model is the historical work of Fisher [6] on the decorated transformation method, proposed

in the 1950s. The improvement of this method is discussed in [7]. Many other quasi-unidimensional Ising-type models were solved using this method [8, 9].

Recently, theoretical investigation of strongly geometrical frustrated materials [10] have been performed, particularly focused on the diamond chain structure, using several numerical approaches [11, 12]. These theoretical results could enhance the other experimental realizations provided by polymeric compounds such as Cu_2OSO_4 [13] and $\text{M}_3(\text{OH})_2$ (with $\text{M} = \text{Ni}, \text{Co}, \text{Mn}$) [14, 15]. Other quasi-unidimensional Heisenberg models were studied using numerical results such as discussed in references [12, 16] and some analytical series expansions have also been performed [17] for similar systems.

The aim of this work is to present the frustrated properties of the asymmetric tetrahedron Ising–Heisenberg (ATIH) chain. This model can be solved exactly by mapping for an effective Ising chain with spins 1/2 or 1 using the method presented by Fisher [6]. This work is organized as follows. In section 2, we present the ATIH chain, considering the Heisenberg interaction with spins 1/2 and 1. In section 3, we discuss the phase diagram at zero temperature showing a rich phase diagram and several critical points, for the spin-(1/2, 1/2) Ising-XYZ chain and spin-(1, 1/2) Ising-XXZ chain. In section 4, we discuss the thermodynamics properties for the Ising–Heisenberg chain with Ising spins $s = 1/2$ or 1 and Heisenberg interaction spins

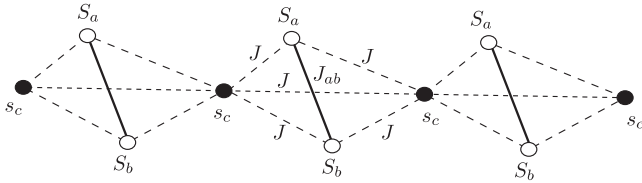


Figure 1. The schematic representation of the coupled asymmetric tetrahedral Ising–Heisenberg chain. All edges (dashed line) of the tetrahedron are represented by the Ising *interaction vertex* except for one (solid line) which is represented by the Heisenberg *interaction edge*.

$S = 1/2$ or 1 . We also considered the correlation function using the decorated transformation method [6]. Finally in section 5 we present our conclusions.

2. The model

The asymmetric tetrahedral Ising–Heisenberg (ATIH) chain is composed of all edges of a tetrahedron (dashed line in figure 1) represented by an Ising-type interaction except for one, which is represented by a Heisenberg-type interaction (solid line in figure 1), which can also be viewed as an Ising–Heisenberg diamond chain. To obtain the ATIH chain we coupled the vertex composed only by the Ising-type *interaction edge*, which we call from now on just the Ising *interaction vertex*, and connected it to another Ising *interaction vertex* of another tetrahedron. On the other hand, the asymmetric edge of the tetrahedron is represented by a Heisenberg type interaction, which we simply call the Heisenberg *interaction edge* (interaction between sites a, b in figure 1).

The schematic representation of the ATIH model is given in figure 1. The Hamiltonian for the ATIH chain discussed above could be written by the following expression:

$$H = \sum_i H_{i,i+1} = \sum_i \left[J (S_{a,i}^z + S_{b,i}^z) (s_{c,i} + s_{c,i+1}) + J_{s_c,i} s_{c,i+1} + H_i^{\text{XYZ}} \right] \quad (1)$$

with $s_{c,i}$ being the spin of the Ising *interaction vertex*, where J is the interaction parameter. The last term included in equation (1) corresponds to the Heisenberg *interaction edge*, which is given by

$$H_i^{\text{XYZ}} = J_x S_{a,i}^x S_{b,i}^x + J_y S_{a,i}^y S_{b,i}^y + J_z S_{a,i}^z S_{b,i}^z, \quad (2)$$

with S_i^v being the spin matrices with $v = x, y, z$ and J_v are their interaction parameters among sites a and b . We can also include the longitudinal external magnetic field in the Hamiltonian (1), which is

$$H_m = \sum_i \left[\frac{h_0}{2} (s_{c,i} + s_{c,i+1}) + h (S_{a,i}^z + S_{b,i}^z) \right], \quad (3)$$

where h_0 is an external magnetic field acting on spin s_c , whereas h is an external magnetic field acting on S_a^z and S_b^z . Note that we are considering different external magnetic fields because we assume that the gyromagnetic factor acting on s_c

could be different from that gyromagnetic factor acting on S_a^z and S_b^z , which we report as $h_0 = gh$ with g being the relative gyromagnetic factor. Equation (1) is a symmetric Hamiltonian in relation to the exchange $s_{c,i} \leftrightarrow s_{c,i+1}$ and $S_{a,i}^z \leftrightarrow S_{b,i}^z$. On the other hand, we note that the Hamiltonian (1) also has an internal spin symmetry $H(s_{c,i}, s_{c,i+1}) = H(-s_{c,i}, -s_{c,i+1})$.

2.1. The XYZ interaction edge with spin-1/2

To perform the partial summation over a decorated site, we need to diagonalize the XYZ *interaction edge* Hamiltonian (2). To evaluate this, we introduce the notations $J_+ = J_x + J_y$ and $J_- = J_x - J_y$. For the spin $S = 1/2$, we obtain the diagonalized Hamiltonian:

$$H_{i,i+1} = \text{diag} \left(\lambda_+^{(1)}, \lambda_+^{(2)}, \lambda_-^{(2)}, \lambda_-^{(1)} \right), \quad (4)$$

where $\text{diag}()$ represents diagonal elements of the Hamiltonian (1), and conveniently we use for simplicity the notation $s_c = s_{c,i}$ and $s'_c = s_{c,i+1}$. Thus the eigenvalues are given by

$$\lambda_{\pm}^{(1)} = \gamma + \frac{1}{4} J_z \pm \frac{1}{4} \sqrt{16\alpha^2 + J_z^2}, \quad (5)$$

$$\lambda_{\pm}^{(2)} = \gamma - \frac{1}{4} J_z \pm \frac{1}{4} J_+,$$

with

$$\alpha \equiv \alpha(s_c, s'_c) = J (s_c^z + s'_c{}^z) + h, \quad (6)$$

$$\gamma \equiv \gamma(s_c, s'_c) = J s_c^z s'_c{}^z + \frac{h_0}{2} (s_c^z + s'_c{}^z), \quad (7)$$

where $\alpha(s_c, s'_c)$ and $\gamma(s_c, s'_c)$ are dependent on the spins s_c and s'_c . Thus we can write them from now on just as α and γ , respectively. Each eigenvalue is given by equation (5) which depends on s_c and s'_c . Then we have 16 eigenvalues.

After diagonalizing the Hamiltonian function we get the corresponding set of eigenvectors also. Thus the new basis is given by

$$|v_1^{(+)}(s_c, s'_c)\rangle = \frac{1}{\sqrt{1+e_1^2}} (e_1 |++\rangle + |--\rangle), \quad (8)$$

$$|v_1^{(-)}(s_c, s'_c)\rangle = \frac{1}{\sqrt{1+e_2^2}} (e_2 |++\rangle + |--\rangle),$$

$$|v_2^{(+)}\rangle = \frac{1}{\sqrt{2}} (|+-\rangle + |-+\rangle), \quad (9)$$

$$|v_2^{(-)}\rangle = \frac{1}{\sqrt{2}} (-|+-\rangle + |-+\rangle),$$

where the factors e_1, e_2 depend on spins s_c and s'_c which are given by the following:

$$e_1 \equiv e_1(s_c, s'_c) = \frac{\sqrt{16\alpha^2 + J_-^2} + 4\alpha}{J_-}, \quad (10)$$

$$e_2 \equiv e_2(s_c, s'_c) = \frac{-\sqrt{16\alpha^2 + J_-^2} + 4\alpha}{J_-},$$

where the normalized eigenvectors $|v_1^{(\pm)}(s_c, s'_c)\rangle$ and $|v_2^{(\pm)}\rangle$ belonging to the eigenvalues $\lambda_1^{(\pm)}$ and $\lambda_2^{(\pm)}$ are given by (5). We also remark that the eigenvectors $|v_2^{(\pm)}\rangle$ are independent of the spins s_c and s'_c or we can say it is fourfold-degenerated.

At this point we would like to comment on the relationships of the $e_1(s_c, s'_c)$ and $e_2(s_c, s'_c)$ factors. From (10), it is not difficult to note that these factors transform one eigenvector of equation (8) into the other one, when we exchange the following values:

$$\left\{ \begin{array}{l} s_c \rightarrow -s_c \\ s'_c \rightarrow -s'_c \\ J_- \rightarrow -J_- \\ h \rightarrow -h \end{array} \right\} \Rightarrow |v_1^{(+)}(s_c, s'_c)\rangle \rightarrow |v_1^{(-)}(s_c, s'_c)\rangle, \quad (11)$$

This property could be valid in a more general situation, even in the presence of an external magnetic field. However, it is important to point out that the eigenvalues of equation (5) does not have a similar transformation. The eigenvalues $\lambda_+^{(1)}$ will always be at higher energy levels than the eigenfunction $\lambda_-^{(1)}$. In the case of null magnetic field ($h = 0, h_0 = 0$) we have these coefficients given by

$$e_1(\pm, \mp) = -e_2(\pm, \mp) = 1, \quad (12)$$

$$e_1(\pm, \pm) = \frac{\sqrt{16J^2 + J_-^2 \pm 4J}}{J_-}, \quad (13)$$

$$e_2(\pm, \pm) = \frac{-\sqrt{16J^2 + J_-^2 \pm 4J}}{J_-}.$$

These properties will be useful when we discuss the phase diagram properties.

2.2. The XXZ interaction edge with spin-1

Now we can consider the XXZ interaction among sites a and b (see figure 1), with the spin $S = 1$ case. We diagonalize the Hamiltonian analogous to the previous case. After diagonalizing, the Hamiltonian depends only on s_c and s'_c :

$$H_{i,i+1} = \text{diag} \left(\lambda_+^{(1)}, \lambda_+^{(2)}, \lambda_+^{(3)}, \lambda_+^{(4)}, \lambda^{(5)}, \lambda_-^{(4)}, \lambda_-^{(3)}, \lambda_-^{(2)}, \lambda_-^{(1)} \right), \quad (14)$$

where $\text{diag}()$ represents diagonal elements of the Hamiltonian (1), whereas the eigenvalues are given by

$$\lambda_{\pm}^{(1)} = \pm 2\alpha + \gamma + J_z, \quad (15)$$

$$\lambda_{\pm}^{(2)} = \pm \alpha + \gamma + \frac{1}{2}J_+, \quad (16)$$

$$\lambda_{\pm}^{(3)} = \pm \alpha + \gamma - \frac{1}{2}J_+, \quad (17)$$

$$\lambda_{\pm}^{(4)} = \gamma - \frac{1}{2}J_z \pm \frac{1}{2}\sqrt{J_z^2 + 2J_+^2}, \quad (18)$$

$$\lambda^{(5)} = \gamma - J_z, \quad (19)$$

where α and γ were already defined by equations (6) and (7).

Now for a complete analysis of the ATIH model, we shall turn our attention to study the XXZ interaction edge for the decorated spin-1. In this situation we have nine eigenvectors after diagonalizing the Hamiltonian, corresponding to the

eigenvalues (15)–(19). Thus the normalized eigenvectors are

$$|u_1^+\rangle = |1, 1\rangle, \quad |u_1^-\rangle = |-1, -1\rangle, \quad (20)$$

$$|u_2^+\rangle = \frac{1}{\sqrt{2}}(|1, 0\rangle + |0, 1\rangle), \quad (21)$$

$$|u_2^-\rangle = \frac{1}{\sqrt{2}}(|0, -1\rangle + |-1, 0\rangle),$$

$$|u_3^+\rangle = \frac{1}{\sqrt{2}}(-|1, 0\rangle + |0, 1\rangle), \quad (22)$$

$$|u_3^-\rangle = \frac{1}{\sqrt{2}}(-|0, -1\rangle + |-1, 0\rangle),$$

$$|u_4^+\rangle = \frac{1}{\sqrt{2+f_1^2}}(|1, -1\rangle + |-1, 1\rangle + f_1|0, 0\rangle), \quad (23)$$

$$|u_4^-\rangle = \frac{1}{\sqrt{2+f_2^2}}(|1, -1\rangle + |-1, 1\rangle + f_2|0, 0\rangle),$$

$$|u_5\rangle = \frac{1}{\sqrt{2}}(-|1, -1\rangle + |-1, 1\rangle), \quad (24)$$

where f_1 and f_2 are respectively given by

$$f_1 = \frac{J_z + \sqrt{J_z^2 + 8J_x^2}}{2J_x}, \quad f_2 = \frac{J_z - \sqrt{J_z^2 + 8J_x^2}}{2J_x}, \quad (25)$$

at which point we have a similar situation as was pointed out in equation (11), i.e. these factors transform as

$$J_z \rightarrow -J_z, \quad J_x \rightarrow -J_x \quad \text{then } |u_4^+\rangle \rightarrow |u_4^-\rangle. \quad (26)$$

Again this conclusion is valid even when an external magnetic field is included.

After rewritten the Heisenberg interaction edge Hamiltonian in the diagonal form we are able to discuss the phase diagram for the whole quasi-unidimensional chain for both cases XYZ interaction edge with spin-1/2 and XXZ interaction edge with spin-1.

3. The phase diagrams of the ATIH chain

3.1. The asymmetric tetrahedral spin-(1/2, 1/2) Ising-XYZ chain

To study the phase diagram of the asymmetric tetrahedral spin-(1/2, 1/2) Ising-XYZ chain we use the diagonalized version of the Hamiltonian presented in previous section 2.1. We would like to note that, for the presently considered model, we have a set of 16 different state vectors. Nevertheless, when the translation and the global spin inversion symmetry are taken into account, we find that only eight state vectors have different phases.

As we mentioned above some state vectors are physically equivalent, for example, the state vectors $|v_1^{(+)}(+, +)\rangle$ and $|v_1^{(+)}(-, -)\rangle$ correspond to the same state when we consider the global spin inversion. Once the eigenvalues satisfy the relations $\lambda_{\pm}^{(1)}(s_c, s'_c) = \lambda_{\pm}^{(1)}(-s_c, -s'_c)$ and $\lambda_{\pm}^{(2)}(s_c, s'_c) = \lambda_{\pm}^{(2)}(-s_c, -s'_c)$, we restrict the eigenvectors to only eight

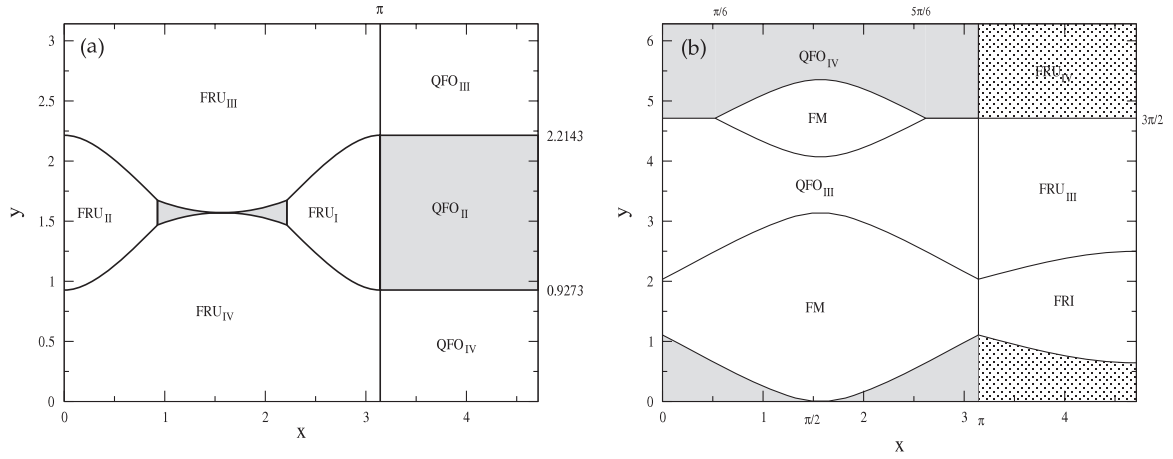


Figure 2. Schematic representation of the phase diagram. (a) For the ATIH chain using the new parameters x and y defined by (35). (b) For the ATIH chain using the new parameters x and y defined by (36).

relevant energy states. So we obtain the following eight states vectors for the asymmetric tetrahedral spin-(1/2, 1/2) Ising-XYZ chain:

$$|QFO_I\rangle = \prod_{k=1}^N \left| +, v_1^{(+)} (+, +) \right\rangle_k, \quad (27)$$

$$m_0 = 0.5, \quad m_1 = \frac{1}{2} \left(\frac{e_1^2 - 1}{e_1^2 + 1} \right)$$

$$|QFO_{II}\rangle = \prod_{k=1}^N \left| +, v_1^{(-)} (+, +) \right\rangle_k, \quad (28)$$

$$m_0 = 0.5, \quad m_1 = \frac{1}{2} \left(\frac{e_2^2 - 1}{e_2^2 + 1} \right)$$

$$|QFO_{III}\rangle = \prod_{k=1}^N \left| +, v_2^{(+)} \right\rangle_k, \quad (29)$$

$$m_0 = 0.5, \quad m_1 = 0,$$

$$|QFO_{IV}\rangle = \prod_{k=1}^N \left| +, v_2^{(-)} \right\rangle_k, \quad (30)$$

$$m_0 = 0.5, \quad m_1 = 0,$$

$$|FRU_I\rangle = \prod_{k=1}^{N/2} \left| +, v_1^{(+)} (+, -), -, v_1^{(+)} (+, -) \right\rangle_k, \quad (31)$$

$$m_0 = 0, \quad m_1 = 0,$$

$$|FRU_{II}\rangle = \prod_{k=1}^{N/2} \left| +, v_1^{(-)} (+, -), -, v_1^{(-)} (+, -) \right\rangle_k, \quad (32)$$

$$m_0 = 0, \quad m_1 = 0,$$

$$|FRU_{III}\rangle = \prod_{k=1}^{N/2} \left| +, v_2^{(+)}, -, v_2^{(+)} \right\rangle_k, \quad (33)$$

$$m_0 = 0, \quad m_1 = 0,$$

$$|FRU_{IV}\rangle = \prod_{k=1}^{N/2} \left| +, v_2^{(-)}, -, v_2^{(-)} \right\rangle_k, \quad (34)$$

$$m_0 = 0, \quad m_1 = 0,$$

where the first element in the product corresponds to the Ising interaction taking two possible values (± 1), and the next

element represents the XYZ *interaction edge* considered in the previous section. All products are carried out over all spin sites. In these relations the single Ising site magnetization m_0 is given for spin-1/2 and m_1 is the single Heisenberg magnetization for the a and b sites (Heisenberg *interaction edge*). The first two states (27) and (28) are new states which arise when we consider the total Ising-XYZ case and their magnetization m_1 depends on the parameters J , J_- and h . These states we will call in general ‘quantum ferromagnetic’ (QFO) states of type I and II, respectively, which are not degenerated and from (8) it is possible to see that the probability of the spin alignment, defined by the functions $e_1(s_c, s'_c)$ and $e_2(s_c, s'_c)$ are not equivalent for the up and down orientations. It is worth remarking that this ‘quantum ferromagnetic’ state could become a quantum ferrimagnetic state when m_1 or m_2 is negative. The energy states of (29) and (30) also have the structure of the first two states but now the probability of the up and down orientations are equivalent: these states are non-degenerate and we can also call these states QFO states of type III and IV, respectively. The states (31)–(34) display four frustrated (FRU) states of types I, II, III and IV, respectively, and are non-degenerate. For these states we use an extended modified unitary cell necessary for the identification of equivalent vector states.

In figure 2, we show the ground-state phase diagram for the system in the absence of the magnetic field ($h = h_0 = 0$). In figure 2(a) let us to consider the following reparameterization for the interaction parameters, without losing any physical generality:

$$\begin{aligned} J &= \sin(x), & J_z &= \sin(y), \\ J_+ &= 4 \cos(y), & J_- &= 4 \cos(x). \end{aligned} \quad (35)$$

Here we represent the interaction parameter by means of two new parameters x and y . For the first two states (equations (27) and (28)) we find that the Heisenberg *interaction edge* magnetization takes the value $m_1 = \sin(x)/2$. Thus for $x = 0, \pi$ we have $m_1 = 0$, and for $x = \pi/2$ we obtain $m_1 = 1/2$.

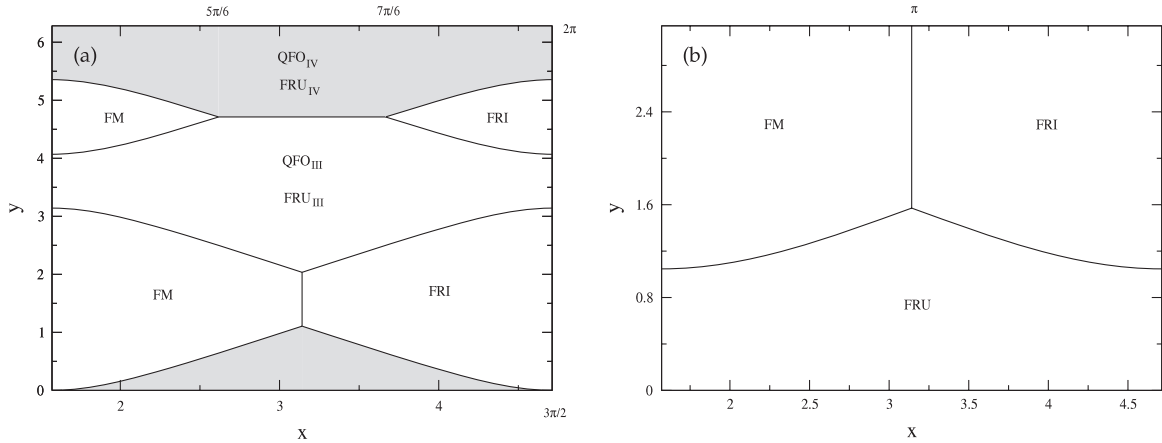


Figure 3. Schematic representation of the phase diagram for the ATI chain, where we consider $\gamma = 0$ and $J_- = 0$. In (a) we display a ferromagnetic (FM) and ferrimagnetic (FRI) state. However, the quantum ferromagnetic (QFO) and the frustrated (FRU) phases are also present. In (b), we fixed the condition $J_x = J_y = J_z$ obtaining only three states' phase energy. The FM, FRI and FRU sectors converges into one tricritical point $(\pi, \pi/2)$.

Certainly, by using this new parameter we restrict the values of interaction parameters as follows: $|J| \leq 1$, $|J_z| \leq 1$ and $|J_{\pm}| \leq 4$. In this limited region we have competing interaction parameters, leading to several ground-state energies. Out of this region there are no new phases.

It is possible to see that, in this phase diagram, we have five tricritical points where three states converge, and two four-critical points where four states converge. In the last case we have that these points are located in the vertical line $x = \pi$. For this position the value obtained from (35) is $J = 0$, $J_z = 0.8$, i.e. in this region the system has pure Heisenberg interaction for a, b sites, and in general, this region is defined by the line where a continuous phase transition occurs. We are able to calculate the other interaction parameters corresponding to these two critical points (x, y) . Thus we have that for the points $(\pi, 0.9273)$ and $(\pi, 2.2143)$ the interaction parameters take the values $J_x = -1.7$, $J_y = 2.3$ and $J_x = -3.2$, $J_y = 0.8$, respectively. In principle we must plot in figure 2(a) the parameters x and y in the interval $[0, 2\pi]$. But in order to highlight the rich region in the interval $[0, \pi]$, we considered it only up to $3\pi/2$ for the x parameter, since we have the continuation of the states QFO_{III}, QFO_{II} and QFO_{IV}. On the other hand, in the y axis we have also repeated states (FRU_I, FRU_{II}, FRU_{IV} and QFO_{II}) which are also present in the interval considered in figure 2(a). We will use the same considerations in the next figures.

In the region where the axis takes the values $x < \pi$, we have that the interaction parameter $J > 0$, i.e. it is positive defined, and for the region $x > \pi$ we obtain a negative value for the parameter $J < 0$. In general, negative values for interaction parameters favor the anti-parallel alignment for the spin-ordered system. Thus we define the type of phase-ordered state by whatever is the FRU or QFO state (left and right side at the axis $x = \pi$ in the diagram). At this stage it is necessary to point out that the phase state QFO_{II} appears in both sectors (gray sector of figure 2(a)). Basically this occurs by the fact that the constant $e_2(s_c, s'_c)$ is different from zero. As will be mentioned below, if the constant $e_2(s_c, s'_c)$ comes close to zero, the region QFO_{II} on the left-hand side disappears.

The other five tricritical points can be found by a simple substitution: for example, the point $(\pi/2, \pi/2)$ is where the phase states FRU_{III}, FRU_{IV} and QFO_{II} coexist. Other tricritical points are $(0.9273, 1.4679)$, $(0.9273, 1.6735)$, $(2.2143, 1.4679)$ and $(2.2143, 1.6735)$.

If we impose the condition $J_x = J_y$, i.e. for the XXZ model, the eight states reduce to seven, six of them will appear in the phase diagram. This is possible because in the limit ($J_- \rightarrow 0$) the constants $e_1(s_c, s'_c)$ and $e_2(s_c, s'_c)$ become 1 and 0, respectively, giving the states FRU_I \rightarrow FRU_{II} as equivalent.

We give in figure 2(b) the ground-state energy for regions resulting from the substitution $J_- = 0$ and where six phases for the ground-state energy are shown. It is easy to see that the states vectors become $|v_1^{(+)}(s_c, s'_c)\rangle \rightarrow |++\rangle$ and $|v_1^{(-)}(s_c, s'_c)\rangle \rightarrow |--\rangle$. For convenience we use the following realization:

$$J = -\sin(x), \quad J_x = 2 \cos(y), \quad J_z = -\sin(y), \quad (36)$$

and now obtain a ferromagnetic (FM) and ferrimagnetic (FRI) state. It is possible to see that the $x = \pi$ axis is still present in these phase configurations. On this line three critical points are shown where four ground states converge. The phase diagram displayed in figure 2 shows several states due to the presence of the $J_{s_c, i s_c, i+1}$ interaction, i.e. the $\gamma(s_c, s'_c)$ term (with $h_0 = 0$) given by (7) allows us to consider this interaction. In [5] the term $J_{s_c, i s_c, i+1}$ was considered null. If we put $\gamma(s_c, s'_c) = 0$ and at the same time impose the equality of some of the interaction parameters, we obtain a very simple phase diagram. This is graphically displayed in figure 3. Figure 3(a) shows that, in the case $\gamma(s_c, s'_c) = 0$, $J_x = J_y$, some states are degenerate, so we identify QFO_{IV} and FRU_{IV} as having the same energy. The same occurs with the QFO_{III} and FRU_{III} states. The FM and FRI states also appear in this diagram. Figure 3(b) shows that, for the case $\gamma(s_c, s'_c) = 0$, $J_x = J_y = J_z$, we obtain the simpler configuration with three phases: the FM, FRI and FRU states. Only one tricritical point where these states converges is present in $(\pi, \pi/2)$. At this

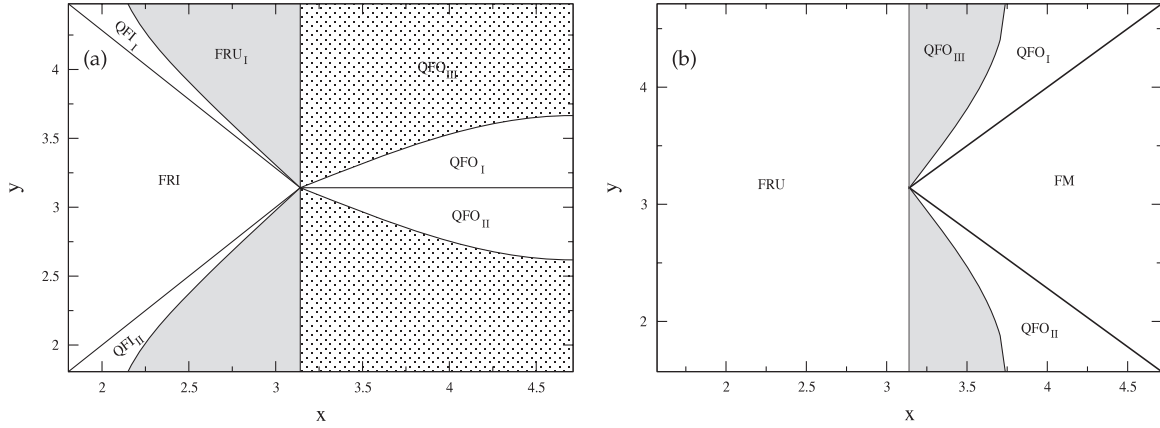


Figure 4. Phase diagram for the ATIH with spin-(1/2, 1) chain. In (a) we have obtained, in a more general case, seven phase diagrams, using the parameters given by equation (37). In (b) we have obtained it, restricting the interaction parameters to $J = J_z = \sin(x)$, $J_x = J_y = 2 \sin(y)$, given by equation (46).

stage we would like to remark that a very similar ground-state configuration was obtained in [5]. However, the realizations used in our work (35) and (36) are different from those used in [5], because we did not include the external magnetic field.

3.2. The asymmetric tetrahedral spin-(1/2,1) Ising-XXZ chain

To obtain all states we need to consider the coupling of the decorated vector states (20)–(24) with the Ising interaction vertex with spin-1/2. This enables us to write down the total vector states of the system. We will restrict the conditions over the interaction parameters without losing generality, using the following values for the interaction parameters:

$$J = -J_z = \sin(x), \quad J_x = 2 \sin(y), \quad (37)$$

in the following we also restrict the system to the case when the external magnetic field is absent ($h_0 = 0, h = 0$). From all possible 24 ground-state energies, which can be obtained from the system, only 15 eigenvalues have different values. In this situation the ground-state eigenvectors for the asymmetric spin-(1/2,1) Ising-XXZ chain, which would appear in the phase diagrams, are given by

$$|\text{FM}\rangle = \prod_{k=1}^N \left| +, u_1^{(+)} \right\rangle_k, \quad m_0 = 0.5, \quad m_1 = 0.5, \quad (38)$$

$$|\text{FRI}\rangle = \prod_{k=1}^N \left| -, u_1^{(+)} \right\rangle_k, \quad m_0 = -0.5, \quad m_1 = 0.5, \quad (39)$$

$$|\text{QFO}_I\rangle = \prod_{k=1}^N \left| +, u_2^{(+)} \right\rangle_k, \quad m_0 = 0.5, \quad m_1 = 0.5, \quad (40)$$

$$|\text{QFO}_{II}\rangle = \prod_{k=1}^N \left| +, u_3^{(+)} \right\rangle_k, \quad m_0 = 0.5, \quad m_1 = 0.5, \quad (41)$$

$$|\text{QFO}_{III}\rangle = \prod_{k=1}^N \left| +, u_4^{(-)} \right\rangle_k, \quad m_0 = 0.5, \quad m_1 = 0, \quad (42)$$

$$|\text{QFI}_I\rangle = \prod_{k=1}^N \left| -, u_2^{(+)} \right\rangle_k, \quad m_0 = -0.5, \quad m_1 = 0.5, \quad (43)$$

$$|\text{QFI}_{II}\rangle = \prod_{k=1}^N \left| -, u_3^{(+)} \right\rangle_k, \quad m_0 = -0.5, \quad m_1 = 0.5, \quad (44)$$

$$|\text{FRU}\rangle = \prod_{k=1}^{N/2} \left| +, u_4^{(-)}, -u_4^{(-)} \right\rangle_k, \quad m_0 = 0 \quad m_1 = 0, \quad (45)$$

where the first element in each product corresponds to the Ising interaction taking two possible values (± 1), and the next element represents the XXZ interaction edge considered in the previous section 2.2. Equation (38) represents a ferromagnetic (FM) state and equation (39) indicates a ferrimagnetic (FRI) state, whereas equations (40)–(42) correspond to quantum ferromagnetic (QFO) states of type I, II and III, respectively. We also have two types of quantum ferrimagnetic (QFI) state given by equations (43) and (44). Finally equation (45) represents a frustrated (FRU) state. All these states given by (38)–(45) are displayed in the phase diagram presented in figure 4(a). It is remarkable that the line $x = \pi$ divides the QFO states from the other ones. Therefore in this case we have a seven-critical point in (π, π) where all states converge.

In order to display the first vector state (38), which was not present in figure 4(a), we change the restriction over the interaction parameters and fixed it as follows:

$$J = J_z = \sin(x), \quad J_x = 2 \sin(y). \quad (46)$$

The phase diagram is given in figure 4(b), where the FM state appears. The other states were already presented in figure 4(a).

Finally it is quite interesting to mention that the state given by equation (38) also appears when the next-nearest interaction parameter considered is null, such as considered in [5], i.e. when $\gamma = 0$, and the restriction is extended over the decorated interaction parameters. For example, if we put

$$J = \frac{1}{5} \sin(x), \quad J_x = J_y = J_z = 4 \sin(y), \quad \gamma = 0, \quad (47)$$

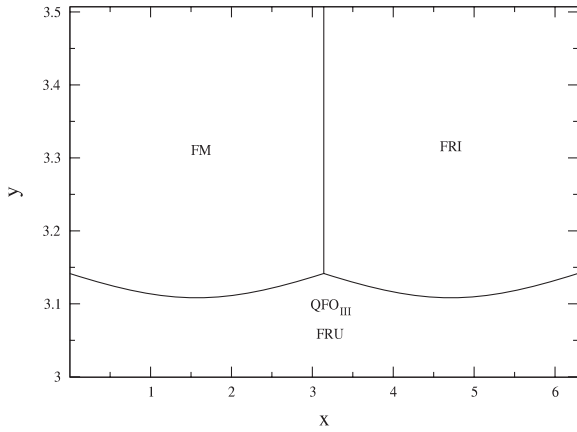


Figure 5. Schematic representation, for the connectors with spin-1/2 and decorated Heisenberg spin-1, of the phase diagram for the decorated XXZ spin-1 model showing the presence of the FM state. We fixed the parameter interaction $J_x = J_y = J_z = 4 \sin(\gamma)$, $J = 1/5 \sin(x)$ and $\gamma = 0$, obtaining only three states. The FM and FRI are non-degenerate while the QFO and FRU are twofold-degenerate. These sectors converge into one tricritical point (π, π) .

we obtain the simpler phase diagram with four states as displayed in figure 5. The FM and the FRI states are separated by the $x = \pi$ line and they end up in QFO_{III} and FRU_I. A similar phase diagram was presented in the work [5] with zero external magnetic field and zero next-nearest interaction parameter. In the work [5] they also consider an external magnetic field but with zero next-nearest interaction parameter where similar phase diagrams were obtained, as displayed in figures 4 and 5(a). So we conclude that the inclusion of the (s_c, s'_c) interaction enables us to investigate a rich number of states even in the absence of an external magnetic field. Both restrictions (46), (47) give the value for the ground-state energy $E_0 = 0$.

4. The ATIH chain thermodynamics

Thermodynamics properties could be studied using the known decorated transformation spin proposed in [6, 7]. Let us write the partition function as follows:

$$\mathcal{Z} = \sum_{\{s_c\}} \prod_{i=1}^N \text{Tr}_{\{S\}} e^{-\beta H_{i,i+1}} = \sum_{\{s_c\}} \prod_{i=1}^N w(s_c, s'_c), \quad (48)$$

where N is the number of decorated bounds, whereas $\text{Tr}_{\{S\}}$ stands for the trace of the central decorated system or Heisenberg *interaction edge* (in our case), while by $w(s_c, s'_c)$ we represent the Boltzmann weight. One should notice that the transformation (48) is rather general, since it is valid for arbitrary spin values contained in the decorated site. The set $\{s_c\}$ represents the Ising *interaction vertex* and would take any spin value too. In this section we study the Ising–Heisenberg chain where the Ising *interaction vertex* takes the spin values $S = 1/2$ or 1.

The ATIH chain partition function can be expressed as

$$\mathcal{Z} = f^N \mathcal{Z}_0, \quad (49)$$

where \mathcal{Z}_0 is the partition function of the effective Ising chain with arbitrary spin- S , whereas f means a constant for the effective Ising chain.

When decorated Heisenberg *interaction edge* sites are occupied by spin-1/2 or 1, it is necessary to perform the partial trace over all those decorated spin sites.

4.1. The Ising interaction vertex with spin-1/2

In order to map the ATIH chain into an effective Ising chain, let us consider the Ising *interaction vertex* with spin-1/2. For this case the associated Boltzmann weight function $w(s_c, s'_c)$ has the form

$$w(s_c, s'_c) = e^{\lambda_+^{(1)}} + e^{\lambda_+^{(2)}} + e^{\lambda_-^{(2)}} + e^{\lambda_-^{(1)}}, \quad (50)$$

where $\lambda_{\pm}^{(1)}$ and $\lambda_{\pm}^{(2)}$ are given by equation (5) for $S = 1/2$ (spin of the decorated sites) whereas the associated Boltzmann weight for spin $S = 1$ could be obtained using equations (15)–(19). Then the ATIH chain model considered here is given by

$$w(s_c, s'_c) = \begin{cases} 2e^{-\beta(\gamma + \frac{1}{4}J_z)} \cosh\left(\beta \frac{1}{4}\sqrt{16\alpha^2 + J_z^2}\right) \\ + 2e^{-\beta(\gamma - \frac{1}{4}J_z)} \cosh\left(\beta \frac{1}{4}J_+\right), & S = 1/2 \\ e^{-\beta\gamma} \left(e^{\beta J_z} + 2e^{\frac{\beta}{2}J_z} \cosh\left(\frac{\beta}{2}\sqrt{J_z^2 + 2J_+^2}\right) \right. \\ + 4 \cosh\left(\frac{\beta}{2}J_+\right) \cosh(\beta\alpha) \\ \left. + 2e^{-\beta J_z} \cosh(\beta 2\alpha) \right), & S = 1. \end{cases} \quad (51)$$

The effective Ising chain partition function is represented by their Boltzmann weight function $\tilde{w}(s_c, s'_c)$ which is

$$\tilde{w}(s_c, s'_c) = f \exp\{-\beta(K s_c s'_c + B(s_c + s'_c))\}. \quad (52)$$

Using a decorated transformation, we obtain the new parameters for the effective Ising chain:

$$\begin{aligned} f^2 &= w\left(\frac{1}{2}, \frac{-1}{2}\right) \sqrt{w\left(\frac{1}{2}, \frac{1}{2}\right) w\left(\frac{-1}{2}, \frac{-1}{2}\right)}, \\ -\beta K &= 4 \ln\left(\frac{w\left(\frac{1}{2}, \frac{1}{2}\right) w\left(\frac{-1}{2}, \frac{-1}{2}\right)}{w\left(\frac{1}{2}, \frac{-1}{2}\right)^2}\right), \\ -\beta B &= \frac{1}{2} \ln\left(\frac{w\left(\frac{1}{2}, \frac{1}{2}\right)}{w\left(\frac{-1}{2}, \frac{-1}{2}\right)}\right), \end{aligned} \quad (53)$$

where the new effective parameters of the Ising chain can be expressed as a function of the parameter of the original Hamiltonian. Thus f is just a constant, whereas K means a coupling parameter and finally B corresponds to the external magnetic field.

The expression for the partition function of the ATIH chain results in

$$\mathcal{Z} = f^N \mathcal{Z}_0 = f^N \sum_{\{s_c\}} \prod_i e^{-\beta(K s_c s'_c + B(s_c + s'_c))}. \quad (54)$$

Using equation (54) we are able to map the asymmetric tetrahedral spin-(1/2, S) Ising–Heisenberg chain into an effective spin-1/2 Ising chain, where the spin- S of the Heisenberg *interaction edge* could be 1/2 or 1.

4.2. The Ising interaction vertex with spin-1

Another case that we consider will be the Ising *interaction vertex* with spin-1. Thus the asymmetric tetrahedral spin (1, S) Ising–Heisenberg chain will be mapped into an effective spin-1 chain. Similar to the previous case we obtain the following Boltzmann weight expressed as follows:

$$\tilde{w}(s_c, s'_c) = f \exp\{-\beta(K_1 s_c s'_c + B(s_c + s'_c) + D(s_c^2 + s_c'^2) + E(s_c^2 s'_c + s_c s_c'^2) + K_2 s_c^2 s_c'^2)\}, \quad (55)$$

where K_1 , K_2 , B , D and E are the parameters to be determined.

The new parameters of equation (55) can be expressed using the associated Boltzmann weight, which is written as

$$f = w(0, 0), \quad (56)$$

$$-\beta K_1 = \frac{1}{4} \ln \left(\frac{w(1, 1)w(-1, -1)}{w(0, 0)^2} \right), \quad (57)$$

$$-\beta B = \frac{1}{2} \ln \left(\frac{w(1, 0)}{w(-1, 0)} \right), \quad (58)$$

$$-\beta D = \frac{1}{2} \ln \left(\frac{w(1, 0)w(-1, 0)}{w(0, 0)^2} \right), \quad (59)$$

$$-\beta E = \frac{1}{4} \ln \left(\frac{w(1, 1)w(1, 0)^2}{w(-1, -1)w(-1, 0)^2} \right), \quad (60)$$

$$-\beta K_2 = \frac{1}{4} \ln \left(\frac{w(1, 1, 1)w(-1, -1)w(0, 0)^2}{w(1, 0)^2 w(-1, 0)^2} \right). \quad (61)$$

Similar to the previous case f means just a constant in the new effective Hamiltonian, while K_1 is the coupling parameter, B corresponds to the external magnetic field, the parameter D represents the single-ion anisotropy, E corresponds to the interaction of the quadratic and linear interactions among the nearest spins and finally K_2 is the parameter of the biquadratic interaction.

In this case if we consider a null magnetic field, we have $w(1, 1) = w(-1, -1)$ and $w(1, 0) = w(-1, 0)$. Under this condition equations (58) and (60) lead to $B = 0$ and $E = 0$, respectively. Then the Boltzmann weight function $w(s_c, s'_c)$ defined by equation (55) reduces the following relation:

$$\tilde{w}(s_c, s'_c) = f \exp \left(-\beta(K_1 s_c s'_c + D(s_c^2 + s_c'^2) + K_2 s_c^2 s_c'^2) \right). \quad (62)$$

Finally we have concluded that our mapping of the asymmetric tetrahedral spin-(1, S) Ising–Heisenberg chain can be expressed as an effective spin-1 Ising chain, where, as before, the spin- S of the Heisenberg *interaction edge* could be 1/2 or 1.

4.3. The ATIH chain correlation functions

We can notice that the partition function of the ATIH chain obtained above, by mapping into the Ising spin chain, is limited. We cannot obtain directly the correlation function because the mapped Ising chain does not depend on the decorated spin. Then we can use the method presented by Fisher [6], where the correlation function for the ATIH chain can be obtained using the decoration transformation in a similar way as was performed for the partition function, assuming we known the correlation function of the effective spin-1 Ising chain.

Using the definition given in [6], we have

$$\langle S_i s_{k_1} s_{k_2} \dots \rangle = \frac{1}{\mathcal{Z}} \sum_{\{s_{k_j}\}} \sum_{S_i} S_i s_{k_1} s_{k_2} \dots e^{-\beta H}, \quad (63)$$

where S_i represents the decorated spin at site i and s_{k_j} are any spins of the systems along the chain. They could be either decorated spins S or undecorated spins s_c , with \mathcal{Z} as the total partition function of the system and H the total Hamiltonian. It is possible to split the above relation in two parts, one being independent of the spin S_i and the other one containing the S_i dependence. Thus we write down the total Hamiltonian (1) as

$$H = H_0(S_i, s_{c,1}, s_{c,2}, \dots) + H_n(s_{c,1}, s_{c,2}, \dots) \equiv H_0 + H_n, \quad (64)$$

where the H_0 contains the dependence of the spins ($S_i, s_{c,1}, s_{c,2}, \dots$) and H_n contains only combinations of the spins ($s_{c,1}, s_{c,2}, \dots$). Actually, in the case when $[H_0, H_n] = 0$, we have

$$\langle S_i s_{k_1} s_{k_2} \dots \rangle = \frac{1}{\mathcal{Z}} \sum_{\{s_{k_j}\}} s_{k_1} s_{k_2} \dots e^{-\beta H_n} \Omega(s_{c,i} s_{c,i+1}), \quad (65)$$

and, as was pointed out by Fisher [6], it is possible to prove that $\Omega(s_{c,i} s_{c,i+1})$ can be represented as

$$\Omega(s_{c,i} s_{c,i+1}) = \sum_{S_i} S_i e^{-\beta H_0}. \quad (66)$$

We give some values for the correlation functions of the asymmetric tetrahedral Ising–Heisenberg model in the case when the Ising *interaction vertex* with spin s_c equal to 1/2 or 1 and the decorated spin could be equal to 1/2 or 1. In the case of spin $s_c = 1/2$, it is possible to obtain an equivalent form [6] for the right-hand side of (66):

$$\Omega(s_{c,i}, s_{c,j}) = (q_0 + q_{0,1}(s_{c,i} + s_{c,j}) + q_{1,1} s_{c,i} s_{c,j}) \sum_{S_i} e^{-\beta H_0}. \quad (67)$$

As an example, let us apply to evaluate the following correlation, with arbitrary sites i and j , instead of performing only among next-nearest sites [5], considering S_a^z could be spin-1/2 or 1. Thus the correlation is

$$\langle S_{a,i}^z s_{c,j} \rangle = q_0 \langle s_{c,j} \rangle + q_{0,1} (\langle s_{c,i} s_{c,j} \rangle + \langle s_{c,i+1} s_{c,j} \rangle) + q_{1,1} \langle s_{c,i} s_{c,i+1} s_{c,j} \rangle \quad (68)$$

where the coefficients q 's can be obtained solving the system equations (65) and (68), from where we verify their solution

is given as a derivative of the parameters obtained in (53) with respect to the magnetic field h , which is

$$q_0 = -\frac{1}{2\beta} \frac{\partial}{\partial h} \ln f, \quad q_{1,0} = \frac{1}{2} \frac{\partial B}{\partial h}, \quad (69)$$

$$\text{and} \quad q_{1,1} = \frac{1}{8} \frac{\partial K}{\partial h}.$$

Then it is possible to write a combination of the correlation function of the effective Ising chain with up to three-body spin correlations. This correlation is given explicitly as follows:

$$\langle s_{c,i} s_{c,j} \rangle = \langle s_c \rangle^2 + (1 - \langle s_c \rangle^2) e^{(i-j)/\xi} \quad (70)$$

$$\langle s_{c,i} s_{c,i+1} s_{c,j} \rangle = \langle s_c \rangle^3 + \langle s_c \rangle (1 - \langle s_c \rangle^2) \times (e^{(i-j)/\xi} + e^{-1/\xi} (1 + e^{(j-i)/\xi})) \quad (71)$$

where ξ is the correlation length of the effective (standard) Ising chain [18].

The autocorrelation function of the $\langle (S_a^z)^2 \rangle$ when we consider the Ising *interaction vertex* $s_c = 1/2$ simply becomes a constant equal to $1/4$, but when we consider spin-1, this expression becomes non-trivial. Analogous to the previous correlation discussed, the general expression can then be

$$\langle (S_{a,i}^z)^2 \rangle = Q_0 + 2Q_{1,0} \langle s_{c,i} \rangle + Q_{1,1} \langle s_{c,i}, s_{c,i+1} \rangle. \quad (72)$$

Once again the coefficients Q 's can be obtained using the following relation:

$$Q_0 = \frac{1}{4} [M(\frac{1}{2}, \frac{1}{2}) + M(-\frac{1}{2}, -\frac{1}{2}) + 2M(\frac{1}{2}, -\frac{1}{2})], \quad (73)$$

$$Q_{1,0} = \frac{1}{2} [M(\frac{1}{2}, \frac{1}{2}) - M(-\frac{1}{2}, -\frac{1}{2})], \quad (74)$$

$$Q_{1,1} = M(\frac{1}{2}, \frac{1}{2}) + M(-\frac{1}{2}, -\frac{1}{2}) - 2M(\frac{1}{2}, -\frac{1}{2}), \quad (75)$$

with

$$M(s_{c,i}, s_{c,i+1}) = \frac{1}{\beta} \frac{\partial w(s_{c,i}, s_{c,i+1})}{\partial J_z} + \frac{1}{2\beta^2} \frac{\partial^2 w(s_{c,i}, s_{c,i+1})}{\partial h^2}, \quad (76)$$

whereas $w(s_{c,i}, s_{c,i+1})$ was already defined in equation (51). Other correlation functions like $\langle S_{a,i}^v S_{b,i}^{v'} \rangle$, are null when $v \neq v'$, whereas for $v = v'$, the correlation function can be obtained directly using the derivatives of the free energy instead of using the previous iterative method such as the one performed by Canova [5]. In particular we show the following nearest correlation:

$$\langle S_a^z \rangle = -\frac{1}{\beta} \frac{\partial \ln(Z)}{\partial h} \quad (77)$$

$$\langle S_{a,i}^v S_{b,i}^v \rangle = -\frac{1}{\beta} \frac{\partial \ln(Z)}{\partial J_v}, \quad \text{with } v = \{x, y, z\}. \quad (78)$$

We remark that the above conclusions are also valid even for spin $s_c = 1$. Similar analysis could be performed to obtain the correlation function when $s_c = 1$. In this case the $\Omega(s_{c,i}, s_{c,i+1})$ function will be defined as

$$\Omega(s_{c,i}, s_{c,j}) = \{q_0 + q_{0,1}(s_{c,i} + s_{c,j}) + q_{1,1} s_{c,i} s_{c,j} + q_{1,2}(s_{c,i} s_{c,j}^2 + s_{c,i}^2 s_{c,j}) + q_{0,2}(s_{c,i}^2 + s_{c,j}^2) + q_{2,2} s_{c,i}^2 s_{c,j}^2\} e^{-\beta H_0}. \quad (79)$$

Using this relation, together with the correlation function of the effective Ising chain with spin-1, we can obtain other

correlations functions for $s_c = 1$, using the same recipes as above.

Alternatively we can obtain this kind of correlation using the direct transfer matrix formalism such as performed in [19]. Meanwhile the advantage of this method could be a non-iterative calculation.

5. Conclusions

The phase diagrams of the asymmetric tetrahedral Ising–Heisenberg (ATIH) chain were studied for the case when the Ising *interaction vertex* is spin-1/2. Firstly we considered the XYZ *interaction edge* with spin-1/2, and null external magnetic field ($h = h_0 = 0$). The diagrams displayed in figure 2(a) have shown seven states appearing in the model, with five critical transition points (x, y) , having three phase states converging, and two critical transition points, where four phase states converge. These states have shown their quantum nature for the XYZ *interaction edge* (decorated sites), for example, for the vector states (27) and (28) we see that up and down orientations in the decorated sites have different probabilities defined by the factors $e_1(s_c, s'_c)$ and $e_2(s_c, s'_c)$. We have also analyzed the particular case when $J_- = 0$, constructing the phase diagram and showing that FM and FRI states appear (figure 2(b)). Other situations have also been studied, in particular the case where $\gamma = 0$, $J_x = J_y$ and for the simpler configuration $\gamma = 0$, $J_x = J_y = J_z$ (figure 3). Secondly, when the XXZ *interaction edge* (decorated) spin is 1, we have also obtained a rich phase diagram for the ground-state energy, even when an external magnetic field and the next-nearest interaction are absent. These phase diagrams are shown in figures 4 and 5. The $x = \pi$ line appears to be the limit of the QFO and the other states, so for the critical point (π, π) the energy takes the value $E_0 = 0$. Some particular cases of our results obtained here have been compared with those obtained in [5].

We have noticed that, using a decorated Ising model mapping transformation, initially given by Fisher [6], the calculation of the partition function for the ATIH chain is reduced to a closed expression of the Ising spin chain. We have considered some particular cases to discuss the thermodynamic properties, such as the Ising *interaction vertex* with spins-1/2 and 1, whereas the interaction edge could be XYZ with spin-1/2 and XXZ with spin-1, respectively. The results for the correlation function are presented generally for the situation when we have the Ising *interaction vertex* with spins-1/2 or 1 and the Heisenberg *interaction edge* with spins-1/2 or 1. We have observed that some correlation function could be obtained using the derivative related to some parameter instead of using the decorated transformation used in [5]. We also considered a long range correlation function where we used the decorated transformation to obtain the result.

Acknowledgments

JSV thanks FAPEMIG for full financial support, OR and SM de S thank CNPq and FAPEMIG for partial financial support.

References

- [1] Escuer A, Vicente R, El Fallah M S, Goher M A S and Mautner F A 1998 *Inorg. Chem.* **37** 4466
- [2] Hagiwara M, Minami K and Katori H A 2001 *Prog. Theor. Phys. Suppl.* **145** 150
- [3] Okamoto K and Ichikawa Y 2002 *J. Phys. Chem. Solids* **63** 1575 see also reference therein
- [4] Strecka J and Jascur M 2004 *J. Magn. Magn. Mater.* **272–276** 984
- [5] Canová L, Strecka J and Jascur M 2006 *J. Phys.: Condens. Matter* **18** 4967
- [6] Fisher M E 1958 *Phys. Rev.* **113** 969
- [7] Domb C and Green M S 1972 *Phase Transitions and Critical Phenomena* vol 1 (New York: Academic)
- [8] Fireman E C and dos Santos R J V 1997 *J. Appl. Phys.* **81** 4198
- [9] Fireman E C, Cressoni J C and dos Santos R J V 2003 *Physica A* **329** 147
- [10] Greedan J E 2001 *J. Mater. Chem.* **11** 37
- [11] Chen S, Wang Y, Ning W Q, Wu C and Lin Q 2006 *Phys. Rev. B* **74** 174424
- [12] Pati S K 2003 *Phys. Rev. B* **67** 184411
- [13] Belaiche M, Drillon M, Aride J, Boukhari A, Biaz T and Legoll P 1991 *J. Chim. Phys. Biol.* **88** 1713
- [14] Guillou N, Pestre S, Livage C and Feret G 2002 *Chem. Commun.* 2358
- [15] Humphrey S M and Wood P T 2004 *J. Am. Chem. Soc.* **126** 13236
- [16] Niggemann H, Uimin G and Zittartz J 1997 *J. Phys.: Condens. Matter* **9** 9031
Niggemann H, Uimin G and Zittartz J 1998 *J. Phys.: Condens. Matter* **10** 5217
- [17] Rojas Onofre, Corraá Silva E V, de Souza S M and Thomaz M T 2004 *Phys. Rev. B* **69** 134405
- [18] Baxter R J 1982 *Exactly Solved Models in Statistical Mechanics* (New York: Academic)
- [19] Valverde J S, Rojas Onofre and de Souza S M 2008 *Physica A* **387** 1947